Received: 8 May 2023 | Accepted: 17 November 2023

DOI: 10.1002/tpg2.20423

The Plant Genome

ORIGINAL ARTICLE

Genetic mapping of dynamic control of leaf angle across multiple canopy levels in maize

Matthew J. Dzievit[1] | **Xianran Li**[2] | **Jianming Yu**[1]

[1]Department of Agronomy, Iowa State University, Ames, Iowa, USA

[2]USDA-ARS, Wheat Health, Genetics, and Quality Research, Pullman, Washington, USA

Correspondence
Jianming Yu, Department of Agronomy, Iowa State University, Ames, IA, USA.
Email: jmyu@iastate.edu

Assigned to Associate Editor Emma Mace.

Funding information
National Institute of Food and Agriculture, Grant/Award Numbers: 2021-67013-33833, Hatch project (1021013); National Science Foundation, Grant/Award Number: IOS-2210259

Abstract

Optimizing leaf angle and other canopy architecture traits has helped modern maize (*Zea mays* L.) become adapted to higher planting densities over the last 60 years. Traditional investigations into genetic control of leaf angle have focused on one leaf or the average of multiple leaves; as a result, our understanding of genetic control across multiple canopy levels is still limited. To address this, genetic mapping across four canopy levels was conducted in the present study to investigate the genetic control of leaf angle across the canopy. We developed two populations of doubled haploid lines derived from three inbreds with distinct leaf angle phenotypes. These populations were genotyped with genotyping-by-sequencing and phenotyped for leaf angle at four different canopy levels over multiple years. To understand how leaf angle changes across the canopy, the four measurements were used to derive three additional traits. Composite interval mapping was conducted with the leaf-specific measurements and the derived traits. A set of 59 quantitative trait loci (QTLs) were uncovered for seven traits, and two genomic regions were consistently detected across multiple canopy levels. Additionally, seven genomic regions were found to contain consistent QTLs with either relatively stable or dynamic effects at different canopy levels. Prioritizing the selection of QTLs with dynamic effects across the canopy will aid breeders in selecting maize hybrids with the ideal canopy architecture that continues to maximize yield on a per area basis under increasing planting densities.

1 | INTRODUCTION

With dwindling amounts of arable land and a growing human population, it is crucial that more food is produced on the same amount of land. Over the last 60 years, maize breeders have developed hybrids that continually maximize the amount of yield per unit of land by maintaining constant yield per plant under high planting density stresses (Duvick et al., 2004; Hammer et al., 2009). Canopy architecture traits like leaf angle and tassel size have changed during this time, as modern hybrids have upright leaf angles and smaller tassels (Duvick et al., 2004; Lambert & Johnson, 1978; Mock & Pearce, 1975). Prior research has established a strong link with this type of canopy architecture and increased light interception and grain yield (Duncan, 1971; Duncan, Williams et al., 1967; Duvick et al., 2004; Lambert & Johnson, 1978; Ma et al., 2014; T. Wang et al., 2011; Xue et al., 2020). Under high planting densities, these traits improve and equalize spatial light distribution across the canopy, improve canopy

Abbreviations: GBS, genotyping-by-sequencing; LA, leaf angle; QTL, quantitative trait locus; SNP, single nucleotide polymorphism.

photosynthesis, and partition more assimilates to the ear (Duvick & Cassman, 1999; Hammer et al., 2009; Lee & Tollenaar, 2007; Xue et al., 2020).

The ideal maize canopy architecture has upright leaf angles in the top canopy that gradually become less upright in the lower canopy (Duncan, Loomis et al., 1967; Zhu et al., 2010). In our previous study, we genetically mapped lower canopy leaf angle by developing two segregating populations using three inbred lines (B73, PHW30, and Mo17) to represent important maize heterotic groups (Dzievit et al., 2019). From these populations, we detected 12 quantitative trait loci (QTLs) for the second leaf below the ear but observed segregation for other leaves in the canopy. Additionally, our meta-analysis of 20 leaf angle genetic mapping studies revealed that most studies used a single leaf or the average of multiple phenotyped leaves, thus making it difficult to determine how these detected regions of the genome contribute to the ideal canopy architecture (Dzievit et al., 2019).

Research across numerous species, including rice, wheat, sorghum, and tomato, have also genetically mapped leaf angle (e.g., Isidro et al., 2012; Z. Li et al., 1999; Nakano et al., 2016; Truong et al., 2015); however, only a few have done so with multiple phenotyped leaves. For example, leaf-specific and canopy-wide QTLs were detected in a rice population phenotyped for tiller angle, flag leaf angle, and leaf angle under the flag leaf (Z. Li et al., 1999). Only a handful of maize studies investigated multiple individual leaves, but these leaves were consecutive rather than spanning the entire plant canopy (e.g., Chang et al., 2016; Chen et al., 2015; Z. Liu et al., 2014; K. Zhang et al., 2020). Furthermore, a study that phenotyped multiple leaves across the canopy only conducted genetic mapping with the average of all leaves in the canopy and the average of leaves above and below the ear (X. Zhang et al., 2017). The few QTLs detected across multiple leaves or levels of the canopy from these studies reported QTL that appear to have varying or similar genetic effects across the canopy. Genetically mapping individual leaves at multiple canopy levels provides us with an opportunity to further explore these two classes of QTLs and determine their impact on developing maize varieties with the ideal canopy architecture.

In this study, we report the discovery of 59 QTLs linked to leaf angle in four different leaves and three derived traits through genetic linkage mapping. We first developed doubled haploid lines in two populations from previously selected F_2 plants (Dzievit et al., 2019) and genotyped these doubled haploid lines using genotyping-by-sequencing (GBS). Four leaves at different canopy levels (Figure 1) were phenotyped for leaf angle across multiple environments. From these measurements, three additional traits were derived to model how leaf angle changes across the canopy. Finally, composite interval mapping was conducted to map QTLs for all seven traits.

Core Ideas

- Leaf angle is an important plant architecture trait in breeding for high planting density.
- Research into the genetic control of leaf angle across multiple canopy levels is limited.
- Genetic mapping discovered many quantitative trait loci (QTLs), with two consistently detected across multiple levels.
- Seven genomic regions were found to contain QTLs with either stable or dynamic effects.

2 | MATERIALS AND METHODS

2.1 | Genetic materials

Inbred lines were developed through the doubled haploid process from previously selected F_2 individuals (Dzievit et al., 2019). Briefly, we phenotyped F_2 plants for leaf angle and selected plants from both phenotypic extremes and near the population average from two biparental populations derived from B73, Mo17, and PHW30, with PHW30 as the common parent. From each selected F_2 plant, 25 $F_{2:3}$ seeds were sent to the Iowa State Doubled Haploid Facility to develop inbred lines. A male inducer was crossed to each F_3 plant. The induced haploid seeds indicated by the morphological marker were planted in trays, injected with colchicine for genome doubling, and transplanted to the field for selfing. A maximum of two doubled haploid lines were selected from each $F_{2:3}$ family that returned selfed seeds, resulting in 309 doubled haploid lines (130 for the B73 population and 179 for the Mo17 population).

2.2 | Phenotyping for leaf angle

Four canopy levels were phenotyped for leaf angle on the parents, hybrids, and doubled haploid lines, starting after all plants completed anthesis. The number of leaves above or below the ear and below the flag leaf (final leaf below the tassel) delineated the leaves that we phenotyped for leaf angle. In total, four canopy levels were phenotyped based on the position of the tassel and ear: "one below flag" (two below the tassel), "three above ear," "one above ear," and "two below ear." These leaves were chosen to capture leaf angle variation across the canopy and avoid referencing specific total

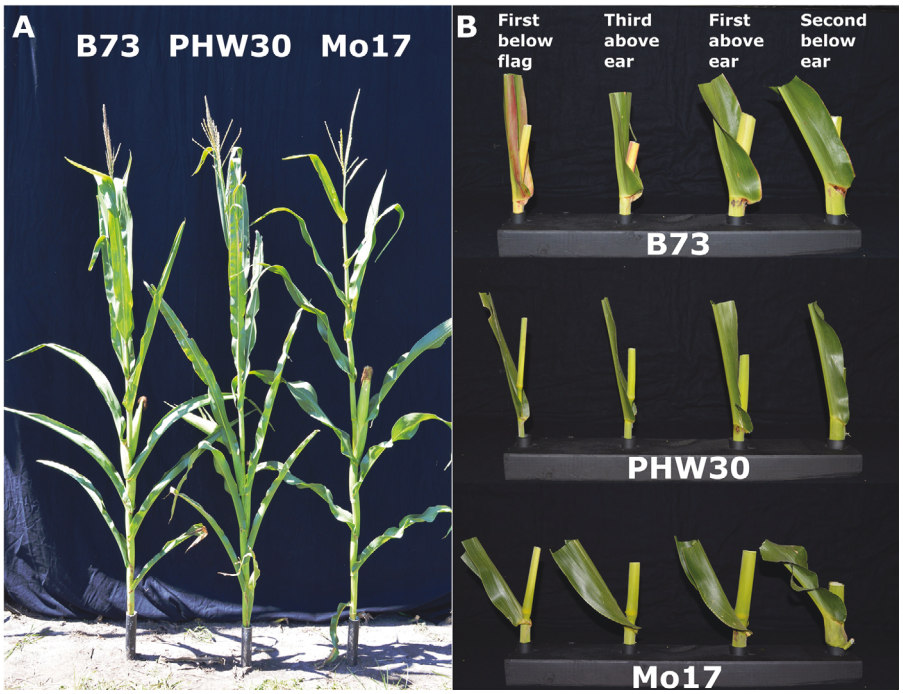

FIGURE 1 Distinct leaf angle architecture for inbred lines B73, Mo17, and PHW30 across different canopy levels. The distinct leaf angle phenotypes (panel A) for B73 (left), PHW30 (middle), and Mo17 (right). Segmented portions of each inbred line in panel B further highlights how leaf angle changes across four levels of the canopy (panel B).

leaf positions that may vary slightly for individuals within a plot, lines, and environments. Leaves with or below the main ear are typically altered due to ear growth and appearance of second ear; leaves lower than "two below ear" are typically senescing at the time of phenotyping. We utilized a digital imaging method (Dzievit et al., 2019) that uses digital images and ImageJ (Schneider et al., 2012) to measure leaf angle for each canopy level. Three representative plants from the middle of each row were chosen, and leaf angle was measured for each plant and canopy level. A digital image was taken for each leaf angle, and ImageJ was then used to measure the angle formed from horizontal and middle of the leaf's mid-rib. The average of all three phenotyped leaves for each canopy level was recorded for each plot. In 2016, leaf angle was only measured for "one below flag" and "two below ear," while all four were measured in 2017 and 2018. To compare results with previous studies, an additional trait, "canopy average," was calculated as the mean of angles for those four measured leaves for 2017 and 2018. Two additional traits were derived from leaf position and leaf angle to model leaf angle variation across the canopy. The canopy level of each phenotyped leaf was assigned a numerical value centered on the ear leaf, which was assigned the 0 position ("one below flag" = 5, "three above ear" = 3, "one above ear" = 1, and "two below ear" = −2). Leaf angle was regressed on canopy level ($y_i = a + bx_i + e_i$, where y_i is the leaf angle value of the ith leaf, x_i is the leaf position, and e_i is the residual). From this regression model, two additional traits were derived for each plot: the intercept a or "canopy intercept" and the slope b or "canopy slope." These two traits were calculated in 2017 and 2018.

2.3 | Experimental design

From 2016–2018, 309 doubled haploid lines were grown at two planting dates using an augmented randomized complete block design (ARCBD). The parents were used as checks for each block and were randomly designated a plot within each block of 32–40 plots (block size depended on year and planting date). The doubled haploid lines from both populations were randomly assigned to the remaining plots across blocks. The first planting date occurred within the first week of May, while the second occurred approximately three weeks after the first. We discarded the second planting date in 2018 due to uneven growth from early-season flooding. The parents and doubled haploid lines were planted at 72,000 seeds per hectare (~29,000 plants per acre) in 5.5-m-long plots spaced 76 cm apart. Additionally, two hybrids (B73 × PHW30 and Mo17 × PHW30) were evaluated under the same conditions and planted only on the first planting date in 2017 and 2018.

Best linear unbiased predictions across environments were obtained for each of the doubled haploid lines. Following previous methods for analyzing an ARCBD (Federer, 1956; Scott & Milliken, 1993; Wolfinger et al., 1997), the following model was fit across environments and populations with SAS

software v9.4 for Windows (SAS Institute, 2018):

$$\begin{aligned} Y_{ijkl} = {} & \text{Env}_i + \text{Block(Env)}_{ij} + \text{Grp} + \text{Grp} \times (\text{Env})_i \\ & + \text{Switch} \times (\text{Grp} \times \text{Pop})_k + \text{Switch} \\ & \times (\text{Grp} \times \text{Pop} \times \text{Env})_{ik} + \text{Switch} \\ & \times \left[\text{Grp} \times \text{Gen}\,(\text{Pop})\right]_{kl} + \text{Switch} \\ & \times \left[\text{Grp} \times \text{Gen}\,(\text{Pop}) \times \text{Env}\right]_{ikl}, \end{aligned}$$

where Env_i is the effect of environment i, Block(Env)_{ij} is the effect of block j nested within environment i, Grp is an auxiliary variable to indicate the groups of checks or two populaions of doubled haploid lines, $\text{Grp} \times (\text{Env})_i$ is the effect of the group within environment i, $\text{Switch} \times (\text{Grp} \times \text{Pop})_k$ is the effect of the population k {1 = B73, 2 = Mo17} and Switch is an indicator variable {0 for checks and 1 for doubled haploid lines}, $\text{Switch} \times (\text{Grp} \times \text{Pop} \times \text{Env})_{ik}$ is the effect of the population k in environment i, $\text{Switch} \times [\text{Grp} \times \text{Gen(Pop)}]_{kl}$ is the effect of genotype l of the population k, and $\text{Switch} \times [\text{Grp} \times \text{Gen(Pop)} \times \text{Env}]_{ikl}$ is the effect ofgenotype l of the population k in environment i. All effects were considered random except Grp effect and Env effect. Trait correlations among all seven traits were calculated within and across the two populations using the Pearson correlation. Additionally, best linear unbiased estimates across environments were obtained for each of the parents, while the calculated mean was recorded for each of the hybrids.

The estimated variance components from the model were used to calculate broad-sense heritability on an entry-mean basis with the following equation:

$$H^2 = \frac{\hat{\sigma}^2_{\text{pop}} + \hat{\sigma}^2_{\text{g}}}{\hat{\sigma}^2_{\text{pop}} + \frac{\hat{\sigma}^2_{\text{pop}\times\text{e}}}{\text{e}_\text{h}} + \hat{\sigma}^2_{\text{g}} + \frac{\hat{\sigma}^2_{\text{ge}}}{\text{e}_\text{h}} + \frac{\hat{\sigma}^2}{\text{e}_\text{h}}},$$

where $\hat{\sigma}^2_{\text{pop}}$ is the estimated between-population genetic variance, $\hat{\sigma}^2_{\text{pop}\times\text{e}}$ is the estimated variance for between-population genetic by environment interaction, $\hat{\sigma}^2_{\text{g}}$ is the estimated within-population genetic variance, $\hat{\sigma}^2_{\text{ge}}$ is the estimated within-population genetic by environment interaction, $\hat{\sigma}^2$ is the estimated error variance, and e_h is the harmonic mean for the environments (Holland et al., 2010; Piepho & Möhring, 2007).

2.4 | Genotyping, filtering, and imputation

To identify QTLs associated with leaf angle variation across the seven traits, 10 leaf punches were taken from a representative plant from each plot. DNA was extracted by a Qiagen DNeasy plant kit for conducting GBS (Elshire et al., 2011) at the University of Minnesota Genomics Center using a 1 × 150 NextSeq rapid sequencing and a previous pipeline for single nucleotide polymorphism (SNP) calling (Dzievit et al., 2019). The resulting SNPs were called based on the B73 RefGen_v4 reference genome.

Segregating SNPs were identified within the parents and allele frequencies from the progeny. The genotype results were stored in a variant call format file (Danecek et al., 2011) and split into different datasets containing B73 doubled haploid lines, Mo17 doubled haploid lines, and parents using TASSEL v5.0 (Bradbury et al., 2007). In addition, we used TASSEL v5.0 to set any genotype call in the doubled haploid lines that were heterozygous to missing. To identify segregating SNPs in the parents, we identified SNP sites through two steps. First, we uplifted previously obtained SNPs for the parents (Dzievit et al., 2019) to RefGen_v4 using CrossMap with the chain file downloaded from Ensembl (Herrero et al., 2016) and identified overlapping SNPs with the current set. Next, we obtained allele frequencies for the progeny using the program "VCFtools v0.1.15" (Danecek et al., 2011). We combined these two SNP sources and estimated genotyping error frequency using an in-house R script with the genotype calls of the new parental data. Together, 77,501 segregating SNPs were identified for the B73 population and 79,026 SNPs for the Mo17 population.

The filtered progeny SNPs were corrected for genotyping errors and imputed. An in-house python (v3.0) script called "VCF_to_MAP-AB" (https://github.com/mdzievit/VCF_to_MAP-AB) was developed to convert a variant call format file to the MAP-AB format used in the genotyping error and correcting suite of tools called "Genotype-Corrector" (GC, Miao et al., 2018, accessed 5/15/2018). After converting to the MAP-AB format with PHW30 labeled as the A allele, each genotype file was pre-processed by removing markers with more than 40% missing data and individuals with more than 80% missing data (GC program "filter_samples_markers.py"). Next, markers with segregation distortion were removed (by testing the Mendelian segregation ratio with a p-value < 0.1 using GC "program preprocess_markers.py"), and consecutive markers within a 150-bp window were combined (GC "program preprocess_markers.py"). The "config-file" was kept with default settings, except the SNP error rate was set for each parent and used to run the "Genotype-Corrector.py" script from GC. Finally, corrected markers were binned (combining adjacent SNPs with the same genotype call) while allowing for one mismatch (GC program "bin_corrected_markers.py"), and any heterozygous calls resulting from the imputation process were set to missing. This process resulted in 3019 bins for the B73 population and 1186 bins for the Mo17 population. The numbers of initial SNPs, informative SNPs, and final bins can be affected by genetic diversity between parental inbreds, and

sequencing and alignment processes. After determining missing data rates for each GE, a total of 32 doubled haploid lines (18 from B73 population and 14 from Mo17) were excluded from genetic mapping because of high missing data.

2.5 | Linkage map construction and genetic mapping

Individual and consensus genetic linkage maps were constructed from the corrected, imputed, and binned genotypic data. Binned genotypic data were formatted for input into the R package "qtl v1.42-8" (Broman et al., 2003). Markers and individuals with more than 10% missing data were removed. A genetic map was initially constructed for each population using the "MSTmap" algorithm (Wu et al., 2008) and implemented with the R package "ASMap v1.0-2" (Taylor & Butler, 2017). Genotyping errors were investigated using the "calc.errorlod" function within "qtl," and genotype calls with scores greater than four were set to missing. The genetic maps were constructed again using the same procedures as previously mentioned and were both approximately 1368.0 cM in length. Finally, the two individual genetic maps were integrated to construct a consensus genetic map 1394.2 cM in length using the R package "Lpmerge v1.6" (Endelman & Plomion, 2014).

The consensus genetic map was used to conduct composite interval mapping for the two populations. Combining our two populations may increase our QTL mapping power; however, it could also cancel out the effect if B73 and Mo17 have opposite effects. For this reason, we chose to keep the two populations separate. Markers from the B73 and Mo17 populations were assigned consensus genetic map positions. The genotypic data files were formatted for input into Windows QTL Cartographer v2.5 (S. Wang et al., 2012), with PHW30 labeled as parent A and coded appropriately. Composite interval mapping with a walk speed of 1 cM, forward and backward regression with an in and out probability of 0.10, and a window size of 10 cM were conducted for each of the seven traits. Permutation testing with 1000 replications was used to identify a trait-specific significance threshold at the 5% level for QTL detection. A positive additive effect for detected QTLs indicates parent A's allele (PHW30) increased leaf angle, while a negative additive effect indicates parent B's allele (B73 or Mo17) increased leaf angle. In addition, a genome-wide single-marker analysis using an *F*-test with physical distance and uncorrected genotypic data was conducted for the seven traits with 37,831 SNPs from the B73 population and 39,922 SNPs from the Mo17 population to corroborate the composite interval mapping results.

3 | RESULTS

3.1 | Phenotype data

Analysis of variance indicated genotype and genotype-by-environment were significant sources of variation for all traits (Table 1; $p < 0.01$), while environment was a significant source of variation for all traits except "canopy slope" (Table 1; $p < 0.01$). Broad-sense heritability on an entry-mean basis was high for all traits and ranged from 0.87 to 0.97 (Table 1).

Phenotypic distributions of the combined best linear unbiased predictors within and across populations were normally distributed across all traits and varied widely (Figure 2). Leaf angle measurements for the four phenotyped leaves were significantly correlated with each other ($p < 0.001$) and consistent across two populations (Figure 2). The strength of the correlation between leaves increased as the distance between them decreased (Figure 2). For example, in the combined population, "one below flag" was strongly correlated with "three above ear" ($r = 0.88$, Figure 2), whereas "one below flag" was only moderately correlated with "second below ear" ($r = 0.41$, Figure 2). This trend was also consistent across both populations (Figure 2).

The three derived traits, "canopy average," "canopy intercept," and "canopy slope," varied in strength of correlation with the measured leaf angle traits. In the combined population, "canopy average" was significantly and positively correlated with all traits ($p < 0.001$), and it had the highest correlation with "one below flag" ($r = 0.90$, Figure 2) among four measured traits. Similarly, "canopy intercept" was also significantly and positively correlated with all traits ($p < 0.001$), and it had the highest correlation with "one above ear" ($r = 0.948$, Figure 2) among four measured traits. On the other hand, "canopy slope" was significantly and positively correlated with all other traits ($p < 0.001$) except for "two below ear," where it was significantly but negatively correlated ($p < 0.05$, $r = -0.13$, Figure 2).

3.2 | Modeling leaf angle across canopy levels

Leaf angle was regressed on canopy level to model how leaf angle fluctuates across the canopy, and it was done for the parents, hybrids, and doubled haploid lines. A strong positive slope was observed for B73, while PHW30 had a slightly positive slope (Table 2). In contrast, Mo17 had a moderately negative slope (Table 2). This trend for the three parents continued in the doubled haploid lines, where doubled haploid lines from the B73 population tended to have positive slopes, whereas those from the Mo17 population tended to have

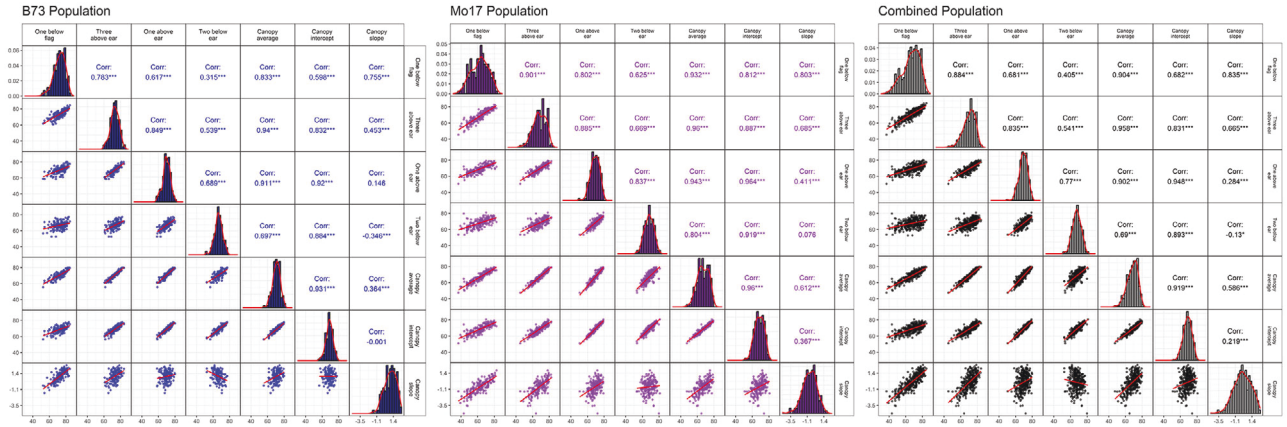

FIGURE 2 Trait correlations between the four phenotyped and three derived leaf angle measurements both within and across populations. Plots on the diagonal line describe the distribution of each measurement. The bottom triangle depicts the scatter plot between the seven measurements, while the upper triangle shows the correlation and significance level (***p-value < 0.001; **p-value < 0.01; and *p-value < 0.05).

negative slopes (Table 2; Figure 3). Overall, doubled haploid lines from the two populations had a similar "canopy intercept" (Table 2), but those from the B73 population tended to have a higher "canopy average" (Table 2).

3.3 | Genetic mapping

Composite interval mapping was conducted separately for each population across all seven traits. Trait-specific significance thresholds ranged from 3.1 to 3.4 logarithm of odds. In total, 59 QTLs were identified in the two populations and were detected on all chromosomes except 9 and 10 (Table S1; Figure 4). In the B73 population, 22 QTLs were detected, while 37 were detected in the Mo17 population (Table S1; Figure 4). The number detected for each trait ranged from five in "three above ear" to 11 in "canopy average" and "one below flag" (Table S1; Figure 4). A single-marker scan with genomic position of unprocessed genotypic data supported these detected QTLs (Figure S1). Additive effects ranged from −0.46 to 0.35 for "canopy slope" and −3.35 to 4.14 for leaf angle traits (Table S1). Additionally, the amount of phenotypic variation explained by the individual QTL ranged from 4.2% to 26.7%, while the total variation explained for each trait ranged from 14.1% to 54.4% (Table S1).

Seven genomic regions were detected across at least four traits, three of which were detected in at least five traits. The genomic region on chromosome 5 was detected across all seven traits in the Mo17 population and has a positive additive effect (Table S1; Figure 4). Another genomic region at 300 Mb on chromosome 1 was detected for five of the seven traits in the Mo17 population and suggestive for two other traits ("three above ear" and "canopy slope") and has a positive additive effect. For the B73 population, only one genomic region at 148 Mb on chromosome 3 was detected for four traits. Among these seven genomic regions, three had QTLs detected for "canopy slope" (Table S1).

Relationships among leaf angle measurements at different positions can be viewed as a form of allometry, which is one aspect for developmental reaction norm (two other aspects being ontogeny and plasticity) (Pigliucci et al., 1996). To reveal the genetics underlying the observed leaf angle variation across the canopy, we plotted the genetic effects of the seven genomic regions (Figure 5; Table S2). Assuming the same loci were underlying these genomic regions, even though the peak signal region varied slightly for some of the QTLs, both dynamic and stable effects across the canopy were observed. The additive effects varied more across different canopy levels for the dynamic QTLs than the stable QTLs. For example, the additive effect range for the QTLs on chromosome 5 was 4.14 for "one below flag" and 1.29 for "two below ear", and it was considered a dynamic QTL. The QTLs on chromosome 1 near 300 Mb had a range of 2.37 for "one below flag" and 1.59 for "two below ear", and it was considered a stable QTL.

When additive effects were regressed on leaf positions, the slopes for three stable QTLs were not significant, agreeing with the non-significance of these three genomic regions for "canopy slope" (Table S2). The slopes for two (chr3:2 Mb and chr3:183–197 Mb) of the four dynamic QTLs were significant, agreeing with the QTLs detection for "canopy slope." The QTL effects of chr3:148 Mb were clearly not following a linear pattern, and the slope were not significant. While the additive effects of chr5:55–90 Mb were not following the linear pattern and the slope was not significant, this QTL was significant for "canopy slope."

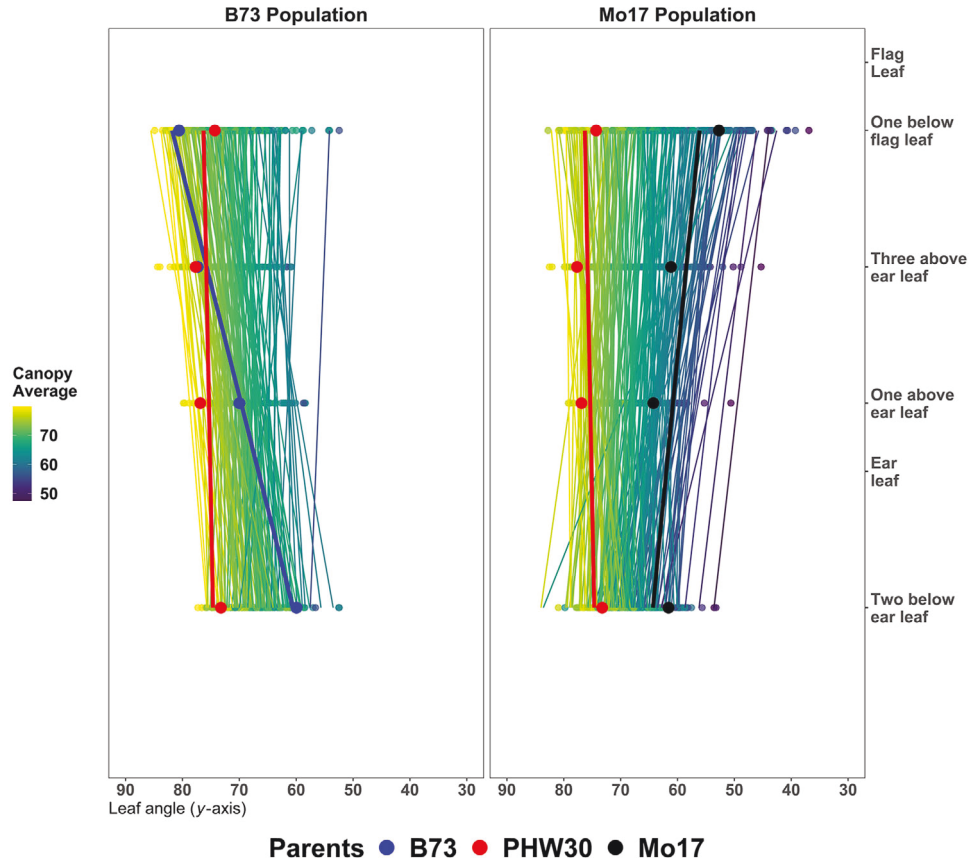

FIGURE 3 Modelling of leaf angle across canopy levels for the three parents and two populations. Four canopy levels were phenotyped for leaf angle and were represented by four leaves based on their distance from the flag (final) or ear leaf. Leaf angle measurements were regressed on the numerical positions of the leaves with the ear leaf positioned as zero. Regression lines are plotted for each genotype and colored according to the overall canopy average (average of all four leaves phenotyped).

4 | DISCUSSION

Simulation and empirical research have determined the ideal canopy architecture for high planting densities should involve upright leaf angles in the upper canopy that gradually transition to less upright in the lower canopy (Duncan, 1971; Long et al., 2006; X. Zhang et al., 2017). This canopy configuration distributes light more efficiently throughout the dense canopy by allowing light to penetrate deeper into the canopy to intercept more light (Duncan, Loomis et al., 1967; Lee & Tollenaar, 2007; Zhu et al., 2010) and contributes to the adaptation to high planting densities seen in the United States and other countries (Duvick et al., 2004; Hammer et al., 2009; Ma et al., 2014; T. Wang et al., 2011). Leaf angle is one of many traits that have contributed to the differential yield response maize hybrids from different decades have shown in the United States and China (Duvick et al., 2004; Ma et al., 2014). While yield responds to different leaf angles and density configurations, the response of leaf angle under various planting densities has been small, less than five degrees from low to high (L. Ku et al., 2016; H. Wang et al., 2017), or limited to specific genetic backgrounds (Pioneer, 2015). While plant density is an important area of research, it was not a main focus of the current study.

Even though the ideal canopy architecture distributes light more efficiently throughout the dense canopy, most previous genetic mapping studies have not investigated leaf angle variation across the canopy (Dzievit et al., 2019; Mantilla-Perez & Salas-Fernandez, 2017). This study followed up on observations made from our recent leaf angle genetic mapping and meta-analysis study. We used doubled haploid lines developed from the populations used in the previous study (Dzievit et al., 2019) to investigate leaf angle variation at four different canopy levels.

Previous research typically used the average of multiple phenotyped leaves for genetic mapping (Ding et al., 2015; L. X. Ku et al., 2010, 2012; L. Ku et al., 2016; C. Li et al., 2015; Lu et al., 2007; Mickelson et al., 2002; X. Zhang et al., 2017); however, few investigated the correlation between multiple phenotyped leaves (Mickelson et al., 2002) or portions of the canopy (X. Zhang et al., 2017). Three representative plants were sampled from the middle of each row and showed little within-row variation (data not shown), thus serving as the best proxy for a canopy-level phenotype. The high

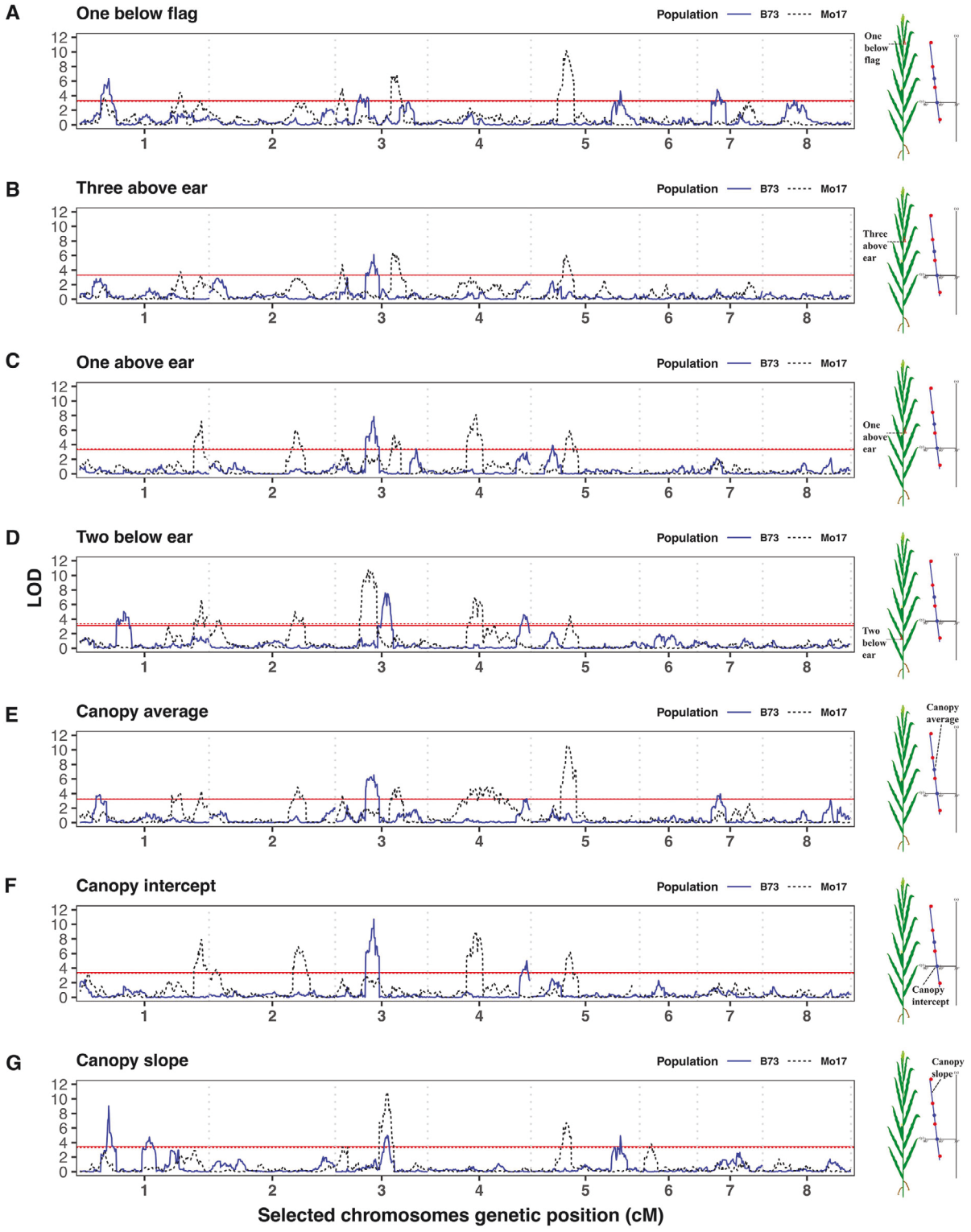

FIGURE 4 Linkage mapping of leaf angle across seven traits. Logarithm of odds plots for selected chromosomes from the composite interval mapping. Results for two populations are combined into each plot for each of the four phenotyped traits (A–D) and three derived traits (E–G). Chromosomes were selected for plotting if they contained a significant quantitative trait locus above the significance threshold among all results. The horizontal red line indicates the trait specific significance threshold and vertical dotted lines separate the selected chromosomes.

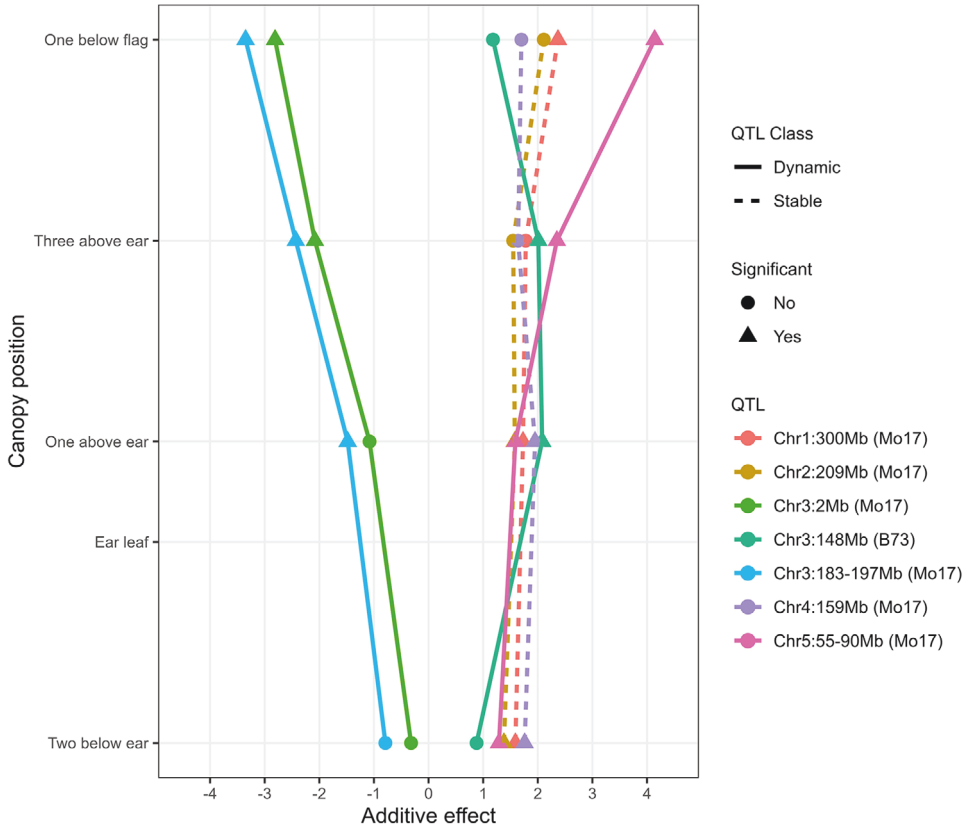

FIGURE 5 Seven quantitative trait loci (QTLs) have either stable or dynamic genetic effects across the canopy. Linkage mapping of leaf angle across seven traits revealed seven consistent QTLs. Dynamic QTLs have different effects depending on the canopy level, whereas stable QTLs have similar effects across the canopy levels.

correlations of "canopy average" with all leaves above the ear (> 0.90) were consistent with previous research (Mickelson et al., 2002). On the other hand, the correlation of "canopy average" with the lower leaf ("two below ear") was smaller (0.69). This was consistent with a similar study that found "canopy average" was less correlated with the average of the lower canopy than the average of the upper canopy (X. Zhang et al., 2017). This suggests that the "canopy average" might not be suitable for representing the lower canopy in genetic mapping, and the upper and lower canopy may be dynamically controlled.

Phenotyping individual leaves at different canopy levels allowed us to investigate the static allometry of leaf angle and unravel its genetic control. Static allometry describes the growth rate between two traits at the same developmental stage. In this study, we calculated a "canopy slope" by phenotyping leaves at different canopy levels at the same developmental stage (after anthesis). This trait explains the rate at which leaf angle changes in relation to canopy level. The three parents used in this study vary in their overall leaf angles and "canopy slope." Inbred line B73 had a configuration close to the ideal canopy. It had upright leaf angles in the upper canopy and slightly less upright in the lower, resulting in a strong positive "canopy slope." On the other hand, Mo17 had relatively flat leaf angles across the canopy and a small negative "canopy slope," meaning the leaf angle became slightly upright lower in the canopy. The "canopy slope" for the common parent, PHW30, was close to 0, indicating a leaf angle throughout the canopy levels. The doubled haploid lines generally followed the trend of the parents, with the B73 population generally having a positive "canopy slope" while the Mo17 generally having a negative "canopy slope." Together, these results suggest different genetic mechanisms may control the rate at which maize plants change leaf angle throughout canopy levels. On the other hand, modeling leaf angle throughout the canopy with a linear model is the initial step in this emerging field, as fitting more complex models will require more datapoints from additional measured leaves in the future. Additional high-throughput measurement and analytic methods are needed to systematically detect QTLs with different effect changes and define different groups of QTL.

Genetic mapping with individual leaves rather than only the average of all phenotyped leaves enabled us to explore leaf angle QTL effects throughout the canopy and begin unraveling the genetic basis of static allometry. Positive or negative genetic effects for the detected QTLs indicate the source of upright leaf angle (positive indicates PHW30, while

TABLE 1 Combined analysis of variance and broad-sense heritability on an entry-mean basis for the doubled haploid populations evaluated across multiple environments.

Trait	Num. Env.	Env.	Block	Pop.	Pop. × Env.	Genotype (Pop.)	Genotype (Pop.) × Env.	Heritability
One below flag	5	4.02**	0.19	46.63	2.01	82.16**	10.52**	0.97
Three above ear	3	17.65**	0.07	11.34	0.19	46.20**	7.22**	0.93
One above ear	3	14.82**	0.22	0.10	0.46	28.22**	6.08**	0.87
Two below ear	5	13.78**	0.23*	0.75	0.80	28.16**	4.18**	0.93
Canopy average	3	25.36**	0.20*	6.79	0.05	36.90**	4.18**	0.96
Canopy intercept	3	20.42**	0.20*	0.00	0.49	27.42**	3.34**	0.93
Canopy slope	3	0.94	0.00	1.39	0.13	1.10**	0.22**	0.92

Within a column, variance estimates with significance levels of $*0.05 > p > 0.01$, $**0.01 > p > 0.001$, and $***p < 0.001$.
Abbreviations: Env., environment; Num. Env., number of environments; Pop., population.

negative indicates either B73 or Mo17). When visualizing the leaf angle QTL effects at the different canopy levels, two classes of leaf angle QTLs emerged: a stable effect across canopy levels and a dynamic effect based on canopy level. The stable effect class is most illustrated by two well-characterized mutants, *liguleless1* and *liguleless2*, that have consistently upright leaves across the canopy (Harper & Freeling, 1996). The QTLs detected on chromosomes 1 (~300 Mb), 2 (~210 Mb), and 4 (~159 Mb) had stable additive effects across the canopy. These three include peaks that did not pass the trait-specific significance thresholds, which could be due to our sample size not being large enough to declare those differences as significant across all leaves in the canopy. Nevertheless, the range of the additive effects within this class of leaf angle QTL was small. The findings suggest these QTLs are affected only to a small degree by spatial or temporal effects.

The QTLs detected with "canopy slope" generally fit into the dynamic effects class. For example, a major-effect QTL with dynamic effects was detected on chromosome 5. Since this QTL included "canopy slope," we suspected the additive effect to be strongest in the upper or lower canopy and weaker in the opposite part of the canopy. The dynamic effects we observed for this locus confirmed our hypothesis. Similar results, but with smaller effects, were observed for two of the QTLs (chr3:2 Mb and chr3:183–197 Mb). Had we only used "canopy average" for genetic mapping, all seven genomic regions would have been detected, but we would not have observed the dynamic effects at different canopy levels. A QTL with similar dynamic effects was detected in a previous study from genetic mapping with averaged leaves from the upper and lower canopy (X. Zhang et al., 2017). Additionally, dynamic effects were observed for cloned genes *ZmCLA4* (J. Zhang et al., 2014) and *ZmTAC1* (L. Ku et al., 2011). Together, these observations suggest that these types of QTLs are developmentally dependent, meaning the structural leaf components influencing leaf angle may degrade over time, with a greater effect in older more developed leaves (lower in the canopy). Phenotyping the same leaves across the growing season may elucidate this matter. Additionally, this class of leaf angle QTL reflects the composition of the ideal canopy architecture under high planting density (upright in the upper canopy and less upright in the lower). For example, an analysis of Chinese hybrids released from the 1950s to the 2000s showed older hybrids with more horizontal and consistent leaf angles, while modern hybrids have the ideal ideotype for high planting densities (Ma et al., 2014). Breeders selecting high-yielding varieties under those conditions may have favored dynamic leaf angle QTL to help maximize canopy light absorption.

Detection of a third class of QTL that only affects a single leaf or portion of the canopy could be possible; however, it is difficult to know whether these are truly leaf-specific or

TABLE 2 Leaf angle phenotypic values for parents, hybrids, and doubled haploid lines.

Group	One below flag	Three above ear	One above ear	Two below ear	Canopy average	Canopy intercept	Canopy slope
B73	80.6 ± 0.33	77.3 ± 0.47	70.0 ± 0.71	60.0 ± 0.49	72.0 ± 0.39	66.7 ± 0.54	3.0 ± 0.12
Mo17	52.7 ± 0.52	61.1 ± 0.68	64.3 ± 0.63	61.6 ± 0.62	59.9 ± 0.45	62.0 ± 0.60	−1.2 ± 0.16
PHW30	74.3 ± 0.28	77.7 ± 0.57	76.9 ± 0.51	73.2 ± 0.24	75.5 ± 0.36	75.1 ± 0.37	0.2 ± 0.06
B73 × PHW30	75.9 ± 0.64	72.1 ± 0.97	68.5 ± 0.90	64.4 ± 1.07	70.3 ± 0.74	67.4 ± 0.78	1.6 ± 0.18
Mo17× PHW30	60.7 ± 1.40	64.1 ± 0.98	67.8 ± 0.76	64.6 ± 0.85	64.2 ± 1.17	65.2 ± 0.89	−0.5 ± 0.22
B73 Population	72.3 ± 0.58 (52.4–84.9)	73.1 ± 0.44 (60.9–84.4)	69.7 ± 0.40 (58.4–79.8)	66.7 ± 0.42 (52.4–77.3)	70.6 ± 0.40 (55.4–79.9)	68.7 ± 0.37 (56.6–77.8)	0.9 ± 0.08 (−1.6 to 2.6)
Mo17 Population	62.6 ± 0.76 (36.9–82.7)	68.3 ± 0.55 (45.3–82.5)	69.1 ± 0.39 (50.6–79.2)	68.0 ± 0.40 (53.2–80.9)	66.8 ± 0.50 (47.5–79.4)	68.3 ± 0.42 (50.8–80.6)	−0.7 ± 0.08 (−4.7 to 1.8)

Note: Values after number are the standard error, and values within parentheses represent the range.

merely cases from the other two classes. Examples of this third class were identified in our study, but the small sample size may have limited our power to detect QTLs in other parts of the canopy. For example, a QTL on chromosome 5 (4.4 Mb) in the B73 population was only detected for "one above ear"; yet a different study, also using B73 as a parent, detected a QTL for "one below flag" in a similar physical position (Tian et al., 2011). Despite this, there is evidence to support our hypothesis that QTLs can control specific leaves or portions of the canopy. The QTL on chromosome 3 (~219.8 Mb) was only detected for "one above ear" in the B73 population and for the same leaf and similar region in a different study (Pan et al., 2017). In addition, a QTL in the same region was detected from our previous study for "two below ear" (Dzievit et al., 2019), thus suggesting leaf or canopy-specific QTL may be possible. Phenotyping leaves at different canopy levels with larger sample sizes may provide more evidence to support the existence of this third class of QTL.

The major QTL on chromosome 5 was supported by multiple studies that phenotyped different leaves throughout the canopy (Chen et al., 2015; C. Li et al., 2015; X. Liu et al., 2019; Pan et al., 2017; Potts, 2014; Tian et al., 2011; X. Zhang et al., 2017). Since most of the studies phenotyped a single leaf or conducted genetic mapping with the average of multiple leaves, it is difficult to see the dynamic canopy effect. The QTL effects for "one below flag" were higher than other leaves in the canopy, which would be expected since we observed the highest variation in that part of the canopy across both populations (Figure 2). The other major QTL on chromosome 1 (~300 Mb) was only supported by a single study that mapped with multiple leaves near the ear (C. Li et al., 2015). Similarly, the consistent QTL on chromosome 2 (~209 Mb) was only supported by a single study that mapped with the average of all leaves in the canopy (X. Zhang et al., 2017). The three derived traits, "canopy average," "canopy slope," and "canopy intercept," co-localized with QTLs identified for phenotyped leaves except for two detected for "canopy slope" on chromosomes 1 (199.7 Mb) and 6 (95.0 Mb). While these were not supported by the phenotyped leaves in this study, they were supported by other studies that phenotyped leaves in multiple parts of the canopy (Chang et al., 2016; C. Li et al., 2015; Pan et al., 2017; Tian et al., 2011; X. Zhang et al., 2017), thus supporting the validity of these QTLs.

Leaf angle-related candidate genes from maize and rice were identified near the overlapping QTLs detected in this study. The major-effect QTLs located between 58 Mb and 90 Mb on chromosome 5 overlaps with the maize ortholog of the rice gene *LC2* (~83 Mb). This rice gene alters the expression of cell division in the lamina joint that affects leaf angle for the upper three rice leaves (S.-Q. Zhao et al., 2010). Additionally, the QTL detected on chromosome 1 near 13.7 Mb is downstream of an orthologous rice gene, *OsMDP1*. It is located at approximately 18.3 Mb and regulates cell-expansion-related genes in the lamina joint of rice (Duan et al., 2006). A recently cloned maize gene, *drl1* (26.7 Mb), is located slightly upstream of the overlapping QTLs on chromosome 1 near 23.5 Mb and controls proper leaf patterning, including restricting auricle expansion at the midrib (Strable et al., 2017). Known mechanisms controlling leaf angle in maize include variation in auricle size (Kong et al., 2017; Strable et al., 2017), while variations in cell size in the lamina joint control leaf angle for rice (Duan et al., 2006; Feng et al., 2016; Gao et al., 2014; Je et al., 2010; Jiang et al., 2012; H. Li et al., 2013). Maize orthologs of similar types of rice genes were also identified for the two consistent QTLs on chromosome 3: *CYP90D2/D2* (4.7 Mb, H. Li et al., 2013) and *LAX* (186.0 Mb, Komatsu et al., 2003). Together, these underlying candidate genes for the consistent QTL support our previous hypothesis regarding the contribution of cell size near the blade and sheath boundary to leaf angle variation in maize (Dzievit et al., 2019).

The progenitors of the doubled haploids developed in this study were previously used for genetic mapping of leaf angle in the lower canopy (Dzievit et al., 2019). Six of the overlapping QTLs previously detected were consistent with the newly detected QTLs, and all but the one on chromosome 8 matched the allele source (Dzievit et al., 2019). The nonmatching additive effects for the QTLs on chromosome 8 were detected in different leaves. Previously, a small positive additive effect and a large dominance effect were detected in the B73 population for the leaf in the lower canopy (Dzievit et al., 2019), whereas in this study, a negative additive effect was detected for "one below flag" in the B73 population. The allelic effect of this locus may depend on the leaf position. Similar results have been obtained when genetic mapping has been conducted with above- and below-canopy averages (X. Zhang et al., 2017).

5 | CONCLUSION

As additional research continues to unravel the genetic control of complex traits, it is imperative that phenotyping efforts are expanded to help us in this process. Our study investigated leaf angle variation across multiple canopy levels (four traits) and three derived traits. For the seven traits, 59 QTLs were uncovered with two major genomic regions detected across multiple canopy levels. Investigating genetic effects at different canopy levels revealed seven genomic regions that can be grouped into two classes of QTLs: stable and dynamic. Stable QTLs had similar effects at different positions of the canopy, while dynamic QTLs had varied effects. Breeders may have inadvertently selected QTLs with dynamic leaf angle effects as they selected inbreds to generate high-performing hybrids under high planting densities. Together, these results further advance our understanding of how leaf angle changes across canopy levels and how targeting QTLs with dynamic effects could contribute to the development of maize hybrids with the ideotype for high planting densities.

AUTHOR CONTRIBUTIONS

Matthew J. Dzievit: Data curation; formal analysis; investigation; methodology; writing—original draft; writing—review and editing. **Xianran Li**: Conceptualization; funding acquisition; investigation; methodology; writing—review and editing. **Jianming Yu**: Conceptualization; funding acquisition; project administration; supervision; writing—review and editing.

ACKNOWLEDGMENTS

This work was supported by the Agriculture and Food Research Initiative competitive grant (2021-67013-33833) and the Hatch project (1021013) from the United State Department of Agriculture National Institute of Food and Agriculture, the National Science Foundation (IOS-2210259), the Iowa State University Raymond F. Baker Center for Plant Breeding, the DuPont Pioneer Graduate Assistantship, and the Iowa State University Plant Sciences Institute. Additionally, the authors would like to thank Gregory Schoenbaum, Rebekah Arnold, Kirsten Backes, Owen Oeltjenbruns, and Alam Ramirez-Reyes for their help in manually measuring leaf angles on the computer.

Open access funding provided by the Iowa State University Library.

CONFLICT OF INTEREST STATEMENT

The authors declare no conflicts of interest.

DATA AVAILABILITY STATEMENT

Data and code used in this study are available in an online public repository: https://github.com/mdzievit/Canopy_LA_Mapping

ORCID

Xianran Li https://orcid.org/0000-0002-4252-6911
Jianming Yu https://orcid.org/0000-0001-5326-3099

REFERENCES

Bradbury, P. J., Zhang, Z., Kroon, D. E., Casstevens, T. M., Ramdoss, Y., & Buckler, E. S. (2007). TASSEL: Software for association mapping of complex traits in diverse samples. *Bioinformatics*, *23*(19), 2633–2635. https://doi.org/10.1093/bioinformatics/btm308

Broman, K. W., Wu, H., Sen, S., & Churchill, G. A. (2003). R/qtl: QTL mapping in experimental crosses. *Bioinformatics*, *19*(7), 889–890. https://doi.org/10.1093/bioinformatics/btg112

Chang, L., He, K., Liu, J., & Xue, J. (2016). Mapping of QTLs for leaf angle in maize under different environments. *Journal of Maize Sciences*, *24*(4), 49–55. https://doi.org/10.13597/j.cnki.maize.science.20160410

Chen, X., Xu, D., Liu, Z., Yu, T., Mei, X., & Cai, Y. (2015). Identification of QTL for leaf angle and leaf space above ear position across different environments and generations in maize (*Zea mays L.*). *Euphytica*, *204*, 395–405. https://doi.org/10.1007/s10681-015-1351-1

Danecek, P., Auton, A., Abecasis, G. R., Albers, C. A., Banks, E., DePristo, M. A., Handsaker, R. E., Lunter, G., Marth, G. T., Sherry, S. T., McVean, G., & Durbin, R. (2011). The variant call format and VCFtools. *Bioinformatics*, *27*(15), 2156–2158. https://doi.org/10.1093/bioinformatics/btr330

Ding, J., Zhang, L., Chen, J., Li, X., Li, Y., Cheng, H., Huang, R., Zhou, B., Li, Z., Wang, J., & Wu, J. (2015). Genomic dissection of leaf angle in maize (*Zea mays* L.) using a four-way cross mapping population. *PloS One*, *10*(10), e0141619. https://doi.org/10.1371/journal.pone.0141619

Duan, K., Li, L., Hu, P., Xu, S. P., Xu, Z. H., & Xue, H. W. (2006). A brassinolide-suppressed rice MADS-box transcription factor, OsMDP1, has a negative regulatory role in BR signaling. *Plant Journal*, *47*(4), 519–531. https://doi.org/10.1111/j.1365-313X.2006.02804.x

Duncan, W. G. (1971). Leaf angles, leaf area, and canopy photosynthesis. *Crop Science*, *11*(4), 482–485. https://doi.org/10.2135/cropsci1971.0011183x001100040006x

Duncan, W. G., Loomis, R. S., Williams, W. A., & Hanau, R. (1967). A model for simulating photosynthesis in plant communities. *Hilgardia*, *38*(4), 181–205. https://doi.org/10.3733/hilg.v38n04p181

Duncan, W. G., Williams, W. A., & Loomis, R. S. (1967). Tassels and the productivity of maize. *Crop Science*, *7*(1), 37–39. https://doi.org/10.2135/cropsci1967.0011183x000700010013x

Duvick, D. N., & Cassman, K. G. (1999). Post–green revolution trends in yield potential of temperate maize in the North-Central United States. *Crop Science*, *39*(6), 1622–1630. https://doi.org/10.2135/cropsci1999.3961622x

Duvick, D. N., Smith, J. S. C., & Cooper, M. (2004). Long-term selection in a commercial hybrid maize breeding program. In J. Janick (Ed.), *Plant breeding reviews: Long-term selection: Crops, animals, and bacteria* (pp. 109–151). John Wiley & Sons, Inc.

Dzievit, M. J., Li, X., & Yu, J. (2019). Dissection of leaf angle variation in maize through genetic mapping and meta-analysis. *The Plant Genome*, *12*(1), 180024. https://doi.org/10.3835/plantgenome2018.05.0024

Elshire, R. J., Glaubitz, J. C., Sun, Q., Poland, J. A., Kawamoto, K., Buckler, E. S., & Mitchell, S. E. (2011). A robust, simple genotyping-by-sequencing (GBS) approach for high diversity species. *PloS One*, *6*(5), e19379. https://doi.org/10.1371/journal.pone.0019379

Endelman, J. B., & Plomion, C. (2014). Lpmerge: An R package for merging genetic maps by linear programming. *Bioinformatics*, *30*(11), 1623–1624. https://doi.org/10.1093/bioinformatics/btu091

Federer, W. T. (1956). Augmented (or hoonuiaku) designs. *Hawaiian Planters' Record*, *55*, 191–208. https://hdl.handle.net/1813/32841

Feng, Z., Wu, C., Wang, C., Roh, J., Zhang, L., Chen, J., Zhang, S., Zhang, H., Yang, C., Hu, J., You, X., Liu, X., Yang, X., Guo, X., Zhang, X., Wu, F., Terzaghi, W., Kim, S. K., Jiang, L., & Wan, J. (2016). *SLG* controls grain size and leaf angle by modulating brassinosteroid homeostasis in rice. *Journal of Experimental Botany*, *67*(14), 4241–4253. https://doi.org/10.1093/jxb/erw204

Gao, Y., Wang, G., Yuan, S., Qin, Y., Zhao, J., Zhang, Y., Zhang, W., & Li, X. (2014). Phenotypic analysis and molecular characterization of an allelic mutant of the *D61*. *The Crop Journal*, *2*(4), 175–182. https://doi.org/10.1016/j.cj.2014.04.003

Hammer, G. L., Dong, Z., McLean, G., Doherty, A., Messina, C., Schussler, J., Zinselmeier, C., Paszkiewicz, S., & Cooper, M. (2009). Can changes in canopy and/or root system architecture explain historical maize yield trends in the U.S. corn belt? *Crop Science*, *49*(1), 299–312. https://doi.org/10.2135/cropsci2008.03.0152

Harper, L., & Freeling, M. (1996). Interactions of *liguleless1* and *liguleless2* function during ligule induction in maize. *Genetics*, *144*(4), 1871–1882.

Holland, J. B., Nyquist, W. E., & Cervantes-Martínez, C. T. (2010). Estimating and interpreting heritability for plant breeding: An update. In J. Janick (Ed.), *Plant breeding reviews* (pp. 9–112). John Wiley & Sons, Inc.

Herrero, J., Muffato, M., Beal, K., Fitzgerald, S., Gordon, L., Pignatelli, M., Vilella, A. J., Searle, S. M. J., Amode, R., Brent, S., Spooner, W., Kulesha, E., Yates, A., & Flicek, P. (2016). Ensembl comparative genomics resources. *Database: The Journal of Biological Databases and Curation*, *2016*, bav096. https://doi.org/10.1093/database/bav096

Isidro, J., Knox, R., Clarke, F., Singh, A., DePauw, R., Clarke, J., & Somers, D. (2012). Quantitative genetic analysis and mapping of leaf angle in durum wheat. *Planta*, *236*(6), 1713–1723. https://doi.org/10.1007/s00425-012-1728-5

Je, B. I., Piao, H. L., Park, S. J., Park, S. H., Kim, C. M., Xuan, Y. H., Park, S. H., Huang, J., Do Choi, Y., An, G., Wong, H. L., Fujioka, S., Kim, M.-C., Shimamoto, K., & Han, C. (2010). *RAV-Like1* maintains brassinosteroid homeostasis via the coordinated activation of *BRI1* and biosynthetic genes in rice. *Plant Cell*, *22*(6), 1777–1791. https://doi.org/10.1105/tpc.109.069575

Jiang, Y., Bao, L., Jeong, S. Y., Kim, S. K., Xu, C., Li, X., & Zhang, Q. (2012). XIAO is involved in the control of organ size by contributing to the regulation of signaling and homeostasis of brassinosteroids and cell cycling in rice. *Plant Journal*, *70*(3), 398–408. https://doi.org/10.1111/j.1365-313X.2011.04877.x

Komatsu, K., Maekawa, M., Ujiie, S., Satake, Y., Furutani, I., Okamoto, H., Shimamoto, K., & Kyozuka, J. (2003). LAX and SPA: Major regulators of shoot branching in rice. *Proceedings of the National Academy of Sciences of the United States of America*, *100*(20), 11765–11770. https://doi.org/10.1073/pnas.1932414100

Kong, F., Zhang, T., Liu, J., Heng, S., Shi, Q., Zhang, H., Wang, Z., Ge, L., Li, P., Lu, X., & Li, G. (2017). Regulation of leaf angle by auricle development in maize. *Molecular Plant*, *10*(3), 516–519. https://doi.org/10.1016/j.molp.2017.02.001

Ku, L., Ren, Z., Chen, X., Shi, Y., Qi, J., Su, H., Wang, Z., Li, G., Wang, X., Zhu, Y., Zhou, J., Zhang, X., & Chen, Y. (2016). Genetic analysis of leaf morphology underlying the plant density response by QTL mapping in maize (*Zea mays L.*). *Molecular Breeding*, *36*(5), 63. https://doi.org/10.1007/s11032-016-0483-x

Ku, L., Wei, X., Zhang, S., Zhang, J., Guo, S., & Chen, Y. (2011). Cloning and characterization of a putative *TAC1* ortholog associated with leaf angle in maize (*Zea mays L.*). *PloS One*, *6*(6), e20621. https://doi.org/10.1371/journal.pone.0020621

Ku, L. X., Zhang, J., Guo, S. L., Liu, H. Y., Zhao, R. F., & Chen, Y. H. (2012). Integrated multiple population analysis of leaf architecture traits in maize (*Zea mays L.*). *Journal of Experimental Botany*, *63*(1), 261–274. https://doi.org/10.1093/jxb/err277

Ku, L. X., Zhao, W. M., Zhang, J., Wu, L. C., Wang, C. L., Wang, P. A., Zhang, W. Q., & Chen, Y. H. (2010). Quantitative trait loci mapping of leaf angle and leaf orientation value in maize (*Zea mays L.*). *Theoretical and Applied Genetics*, *121*(5), 951–959. https://doi.org/10.1007/s00122-010-1364-z

Lambert, R. J., & Johnson, R. R. (1978). Leaf angle, tassel morphology, and the performance of maize hybrids. *Crop Science*, *18*, 499–502. https://doi.org/10.2135/cropsci1978.0011183x001800030037x

Lee, E. A., & Tollenaar, M. (2007). Physiological basis of successful breeding strategies for maize grain yield. *Crop Science*, *47*, S-202–S-215. https://doi.org/10.2135/cropsci2007.04.0010IPBS

Li, C., Li, Y., Shi, Y., Song, Y., Zhang, D., Buckler, E. S., Zhang, Z., Wang, T., & Li, Y. (2015). Genetic control of the leaf angle and leaf orientation value as revealed by ultra-high density maps in three connected maize populations. *PloS One*, *10*(3), e0121624. https://doi.org/10.1371/journal.pone.0121624

Li, H., Jiang, L., Youn, J.-H., Sun, W., Cheng, Z., Jin, T., Ma, X., Guo, X., Wang, J., Zhang, X., Wu, F., Wu, C., Kim, S.-K., & Wan, J. (2013). A comprehensive genetic study reveals a crucial role of CYP90D2/D2 in regulating plant architecture in rice (*Oryza sativa*). *New Phytologist*, *200*(4), 1076–1088. https://doi.org/10.1111/nph.12427

Li, Z., Paterson, A. H., Pinson, S. R. M., & Stansel, J. W. (1999). RFLP facilitated analysis of tiller and leaf angles in rice (*Oryza sativa L.*). *Euphytica*, *109*(2), 79–84. https://doi.org/10.1023/A:1003533001014

Liu, X., Hao, L., Kou, S., Su, E., Zhou, Y., Wang, R., Mohamed, A., Gao, C., Zhang, D., Li, Y., Li, C., Song, Y., Shi, Y., Wang, T., & Li, Y. (2019). High-density quantitative trait locus mapping revealed genetic architecture of leaf angle and tassel size in maize. *Molecular Breeding*, *39*(1), Article 7. https://doi.org/10.1007/s11032-018-0914-y

Liu, Z., Yu, T.-T., Mei, X.-P., Chen, X.-N., Wang, G.-Q., Wang, J.-G., Liu, C.-X., Wang, X., & Cai, Y.-L. (2014). QTL mapping for leaf angle and leaf space above ear position in maize (*Zea mays L.*). *Journal of Agricultural Biotechnology*, *22*(2), 177–187. https://doi.org/10.3969/j.issn.1674-7968.2014.02.006

Long, S. P., Zhu, X.-G., Naidu, S. L., & Ort, D. R. (2006). Can improvement in photosynthesis increase crop yields? *Plant, Cell & Environment*, *29*(3), 315–330. https://doi.org/10.1111/j.1365-3040.2005.01493.x

Lu, M., Zhou, F., Xie, C., Li, M., Xu, Y., Warburton, M., & Zhang, S. (2007). Construction of a SSR linkage map and mapping of quantitative trait loci (QTL) for leaf angle and leaf orientation with an elite maize hybrid. *Hereditas*, *29*(09), 1131–1138. https://doi.org/10.1360/yc-007-1131

Ma, D. L., Xie, R. Z., Niu, X. K., Li, S. K., Long, H. L., & Liu, Y. E. (2014). Changes in the morphological traits of maize genotypes in China between the 1950s and 2000s. *European Journal of Agronomy*, *58*, 1–10. https://doi.org/10.1016/j.eja.2014.04.001

Mantilla-Perez, M. B., & Salas-Fernandez, M. G. (2017). Differential manipulation of leaf angle throughout the canopy: Current status and prospects. *Journal of Experimental Botany*, *68*, 5699–5717. https://doi.org/10.1093/jxb/erx378

Miao, C., Fang, J., Liang, P., Zhang, X., Schnable, J. C., & Tang, H. (2018). Genotype-Corrector: Improved genotype calls for genetic mapping. *Scientific Reports*, *8*, 10088. https://doi.org/10.1038/s41598-018-28294-0

Mickelson, S. M., Stuber, C. S., Senior, L., & Kaeppler, S. M. (2002). Quantitative trait loci controlling leaf and tassel traits in a B73 × MO17 population of maize. *Crop Science*, *42*(6), 1902–1909. https://doi.org/10.2135/cropsci2002.1902

Mock, J. J., & Pearce, R. B. (1975). An ideotype of maize. *Euphytica*, *24*(3), 613–623. https://doi.org/10.1007/BF00132898

Nakano, H., Sasaki, K., Mine, Y., Takahata, K., Lee, O., & Sugiyama, N. (2016). Quantitative trait loci (QTL) controlling plant architecture traits in a *Solanum lycopersicum* × *S. pimpinellifolium* cross. *Euphytica*, *211*(3), 353–367. https://doi.org/10.1007/s10681-016-1744-9

Pan, Q., Xu, Y., Li, K., Peng, Y., Zhan, W., Li, W., Li, L., & Yan, J. (2017). The genetic basis of plant architecture in 10 maize recombinant inbred line populations. *Plant Physiology*, *175*(October), 858–873. https://doi.org/10.1104/pp.17.00709

Piepho, H.-P., & Möhring, J. (2007). Computing heritability and selection response from unbalanced plant breeding trials. *Genetics*, *177*(3), 1881–1888. https://doi.org/10.1534/genetics.107.074229

Pigliucci, M., Schlichting, C. D., Jones, C. S., & Schwenk, K. (1996). Developmental reaction norms: The interactions among allometry, ontogeny and plasticity. *Plant Species Biology*, *11*, 69–85. https://doi.org/10.1111/j.1442-1984.1996.tb00110.x

Pioneer. (2015). *Corn leaf angle response to plant density*. https://www.pioneer.com/us/agronomy/corn-leaf-angle-response-plant-density.html

Potts, S. (2014). *Identification of QTL and candidate genes for plant density* [Doctoral dissertation, University of Illinois at Urbana-Champaign]. http://hdl.handle.net/2142/49814

SAS Institute. (2018). *SAS 9.4*. SAS Institute Inc. https://www.sas.com/en_us/learn/academic-programs/software.html

Schneider, C. A., Rasband, W. S., & Eliceiri, K. W. (2012). NIH Image to ImageJ: 25 Years of image analysis. *Nature Methods*, *9*(7), 671–675. https://doi.org/10.1038/nmeth.2089

Scott, R. A., & Milliken, G. A. (1993). A SAS program for analyzing augmented randomized complete-block designs. *Crop Science*, *33*(4), 865–867. https://doi.org/10.2135/cropsci1993.0011183x003300040046x

Strable, J., Wallace, J. G., Unger-Wallace, E., Briggs, S., Bradbury, P., Buckler, E. S., & Vollbrecht, E. (2017). Maize *YABBY* genes *drooping leaf1* and *drooping leaf2* regulate plant architecture. *The Plant Cell*, *29*(July), 1622–1641. https://doi.org/10.1105/tpc.16.00477

Taylor, J., & Butler, D. (2017). R package ASMap : Efficient genetic linkage map construction and diagnosis. *Journal of Statistical Software*, *79*(6), 1–29. https://doi.org/10.18637/jss.v079.i06

Tian, F., Bradbury, P. J., Brown, P. J., Hung, H., Sun, Q., Flint-Garcia, S. A., Rocheford, T. R., McMullen, M. D., Holland, J. B., & Buckler, E. S. (2011). Genome-wide association study of leaf architecture in the maize nested association mapping population. *Nature Genetics*, *43*(2), 159–162. https://doi.org/10.1038/ng.746

Truong, S. K., McCormick, R. F., Rooney, W. L., & Mullet, J. E. (2015). Harnessing genetic variation in leaf angle to increase productivity of *Sorghum bicolor*. *Genetics*, *201*(3), 1229–1238. https://doi.org/10.1534/genetics.115.178608

Wang, H., Liang, Q., Li, K., Hu, X., Wu, Y., Wang, H., Liu, Z., & Huang, C. (2017). QTL analysis of ear leaf traits in maize (*Zea mays* L.) under different planting densities. *The Crop Journal*, *5*(5), 387–395. https://doi.org/10.1016/j.cj.2017.05.001

Wang, S., Basten, C. J., & Zeng, Z.-B. (2012). *WindowsQTL cartographer V2.5_011*. North Carolina State University. https://brcwebportal.cos.ncsu.edu/qtlcart/WQTLCart.htm

Wang, T., Ma, X., Li, Y., Bai, D., Liu, C., Liu, Z., Tan, X., Shi, Y., Song, Y., Carlone, M., Bubeck, D., Bhardwaj, H., Jones, E., Wright, K., & Smith, S. (2011). Changes in yield and yield components of single-cross maize hybrids released in China between 1964 and 2001. *Crop Science*, *51*(2), 512–525. https://doi.org/10.2135/cropsci2010.06.0383

Wolfinger, R. D., Federer, W. T., & Cordero-Brana, O. (1997). Recovering information in augmented designs, using SAS PROC GLM and PROC MIXED. *Agronomy Journal*, *89*(6), 856–859. https://doi.org/10.2134/agronj1997.00021962008900060002x

Wu, Y., Bhat, P. R., Close, T. J., & Lonardi, S. (2008). Efficient and accurate construction of genetic linkage maps from the minimum spanning tree of a graph. *PLoS Genetics*, *4*(10), e1000212. https://doi.org/10.1371/journal.pgen.1000212

Xue, J., Qi, B., Ma, B., Li, B., & Gou, L. (2020). Effect of altered leaf angle on maize stalk lodging resistance. *Crop Science*, *61*, 689–703. https://doi.org/10.1002/csc2.20284

Zhang, J., Ku, L. X., Han, Z. P., Guo, S. L., Liu, H. J., Zhang, Z. Z., Cao, L. R., Cui, X. J., & Chen, Y. H. (2014). The ZmCLA4 gene in the qLA4-1 QTL controls leaf angle in maize (*Zea mays* L.). *Journal*

of Experimental Botany, *65*(17), 5063–5076. https://doi.org/10.1093/jxb/eru271

Zhang, K., Lv, X., Li, F., Wang, J., Yu, H., Li, J., Du, W., Diao, Y., Wang, J., & Weng, J. (2020). Genetic mapping of quantitative trait locus for the leaf morphological traits in a recombinant inbred line population by ultra-high–density maps across multi-environments of maize (*Zea mays*). *Plant Breeding*, *139*, 107–118. https://doi.org/10.1111/pbr.12749

Zhang, X., Huang, C., Wu, D., Qiao, F., Li, W., Duan, L., Wang, K., Xiao, Y., Chen, G., Liu, Q., Xiong, L., Yang, W., & Yan, J. (2017). High-throughput phenotyping and QTL mapping reveals the genetic architecture of maize plant growth. *Plant Physiology*, *173*(3), 1554–1564. https://doi.org/10.1104/pp.16.01516

Zhao, S.-Q., Hu, J., Guo, L.-B., Qian, Q., & Xue, H.-W. (2010). Rice leaf inclination2, a VIN3-like protein, regulates leaf angle through modulating cell division of the collar. *Cell Research*, *20*(8), 935–947. https://doi.org/10.1038/cr.2010.109

Zhu, X.-G., Long, S. P., & Ort, D. R. (2010). Improving photosynthetic efficiency for greater yield. *Annual Review of Plant Biology*, *61*(1), 235–261. https://doi.org/10.1146/annurev-arplant-042809-112206

SUPPORTING INFORMATION

Additional supporting information can be found online in the Supporting Information section at the end of this article.

How to cite this article: Dzievit, M. J., Li, X., & Yu, J. (2023). Genetic mapping of dynamic control of leaf angle across multiple canopy levels in maize. *The Plant Genome*, e20423. https://doi.org/10.1002/tpg2.20423